

1 A transgenic zebrafish line for in vivo visualisation of neutrophil myeloperoxidase.

2

3 Kyle D. Buchan¹, Tomasz K. Prajsnar¹, Nikolay V. Ogryzko^{1,3}, Nienke W.M. de
4 Jong², Michiel van Gent², Julia Kolata², Simon J. Foster⁴, Jos A.G. van Strijp²,
5 Stephen A. Renshaw¹

6 1. The Bateson Centre and Department of Infection, Immunity and Cardiovascular Disease, University
7 of Sheffield, Western Bank, Sheffield, S10 2TN, UK.

8 2. Department of Medical Microbiology, University Medical Center Utrecht, Utrecht University, Utrecht,
9 The Netherlands.

10 3. Centre for Inflammation Research, University of Edinburgh, Edinburgh, EH16 4TJ, United Kingdom.

11 4. Department of Molecular Biology and Biotechnology, University of Sheffield, Western Bank,
12 Sheffield, S10 2TN, UK.

13

14

15 Address for correspondence:

16 Stephen A. Renshaw

17 The Bateson Centre

18 University of Sheffield

19 Western Bank

20 Sheffield

21 S10 2TN, UK.

22

23 Email: s.a.renshaw@sheffield.ac.uk

24 Tel: 0114 2222334

25 Abstract

26

27 The neutrophil enzyme myeloperoxidase (MPO) is a major enzyme made by
28 neutrophils to generate antimicrobial and immunomodulatory compounds, notably
29 hypochlorous acid (HOCl), amplifying their capacity for destroying pathogens and
30 regulating inflammation. Despite its roles in innate immunity, the importance of MPO
31 in preventing infection is unclear, as individuals with MPO deficiency are
32 asymptomatic with the exception of an increased risk of candidiasis. Dysregulation of
33 MPO activity is also linked with inflammatory conditions such as atherosclerosis,
34 emphasising a need to understand the roles of the enzyme in greater detail.
35 Consequently, new tools for investigating granular dynamics *in vivo* can provide
36 useful insights into how MPO localises within neutrophils, aiding understanding of its
37 role in preventing and exacerbating disease. The zebrafish is a powerful model for
38 investigating the immune system *in vivo*, as it is genetically tractable, and optically
39 transparent.

40 To visualise MPO activity within zebrafish neutrophils, we created a genetic
41 construct that expresses human MPO as a fusion protein with a C-terminal
42 fluorescent tag, driven by the neutrophil-specific promoter *lyz*. After introducing the
43 construct into the zebrafish genome by Tol2 transgenesis, we established the
44 *Tg(lyz:Hsa.MPO-mEmerald,cm1c2:EGFP)sh496* line, and confirmed transgene
45 expression in zebrafish neutrophils. We observed localisation of MPO-mEmerald
46 within a subcellular location resembling neutrophil granules, mirroring MPO in human
47 neutrophils. In Spotless (*mpx^{NL144}*) larvae - which express a non-functional zebrafish
48 myeloperoxidase - the MPO-mEmerald transgene does not disrupt neutrophil

49 migration to sites of infection or inflammation, suggesting that it is a suitable line for
50 the study of neutrophil granule function.

51 We present a new transgenic line that can be used to investigate neutrophil
52 granule dynamics *in vivo* without disrupting neutrophil behaviour, with potential
53 applications in studying processing and maturation of MPO during development.

54 Introduction

55

56 The enzyme Myeloperoxidase (MPO) enhances the microbicidal potential of
57 neutrophils by converting hydrogen peroxide (H_2O_2) into the highly toxic antimicrobial
58 compound hypochlorous acid (HOCl) (1), and by forming radicals by oxidating
59 substrates including phenols, nitrate and tyrosine residues (2). MPO is located in the
60 primary granules of neutrophils, which deliver MPO and other bactericidal
61 compounds to invading pathogens by fusing with phagocytic vesicles, accelerating
62 pathogen destruction. MPO is the most abundant protein in the primary granules of
63 human neutrophils (3), and consequently neutrophils are able to produce high levels
64 of HOCl to deliver a potent antimicrobial response that is capable of killing a broad
65 variety of major pathogens (4–6).

66 Importantly, due to the activity of upstream NADPH oxidase, the phagocytic
67 vacuole is thought to be relatively alkaline (~pH 9), and under such conditions MPO
68 activity may be less efficient (7) than other neutrophil enzymes (8). MPO activity
69 appears to be context-dependent, particularly during phagocytosis of large structures
70 such as fungal hyphae (9) or bacterial biofilms (10). In these cases, the phagocytic
71 vacuole does not fully close (11), causing MPO to act at the acidic pH of sites of
72 inflammation (~pH 6) (12), at which it can function normally. This observation is
73 supported by the fact that MPO is thought to play a role in the generation of
74 neutrophil extracellular traps (NETs) (13), which are often induced in response to
75 large targets (14). While the precise site of action of MPO is uncertain, it is clear that
76 it plays a role in antimicrobial defence, as pathogens produce specific virulence
77 factors targeting it (15).

78 Beyond its role in bolstering the antimicrobial defence, MPO is also an
79 important regulator of inflammation. The arrival of neutrophils at the wound site
80 marks the initial steps of the anti-inflammatory response, as MPO is delivered to the
81 wound site to consume H₂O₂ and reduce inflammatory signalling (16,17). There is
82 also a link between aberrant MPO activity and inflammatory conditions: overactivity
83 is associated with cardiovascular disease, multiple sclerosis and glomerulonephritis
84 (18–20), while MPO deficiency has been implicated in pulmonary fibrosis and
85 atherosclerosis (21,22), highlighting its critical role in immune homeostasis. MPO
86 deficiency is a relatively common condition affecting 1 in every 2,000-4,000 people
87 across Europe and North America (23), with no major health risks apart from a
88 susceptibility to *Candida albicans* infections (24). This observation is in stark contrast
89 to people with chronic granulomatous disease (CGD), who lack a working NADPH
90 oxidase. Those with CGD are unable to generate an effective phagocytic
91 environment capable of destroying microbes (25,26). Unlike MPO deficiency, those
92 with CGD experience frequent life-threatening infections from a wide range of
93 pathogens (27), and consequently, the role of MPO is less clear when observed in
94 the context of other oxidative enzymes and compounds. Further studies are required
95 to understand the complex roles of MPO in the immune system.

96 The zebrafish is a powerful model for studying physiology and pathology *in*
97 *vivo* and has been used to model many important conditions ranging from
98 neurodegenerative disorders such as Alzheimer's disease (28), to cancers including
99 melanoma (29) and leukaemia (30). They are optically transparent, making them
100 amenable to imaging studies and produce high numbers of offspring, which permits
101 the application of high-throughput approaches. Another major advantage of the
102 zebrafish is their genetic tractability, facilitating the introduction of large genetic

103 constructs into the genome, often expressing fluorescent proteins driven by tissue-
104 specific promoters (31). Several studies have utilised these features to create
105 transgenic lines labelling macrophages (32) and neutrophils (33) to image the innate
106 immune response during infection (34) and inflammation (35).

107 MPO can be measured using a variety of cytochemical and cytometry-based
108 approaches (36), however there are relatively few tools that allow granular MPO to
109 be visualised *in vivo* and in real time. Mouse models that permit imaging of
110 neutrophil granules and MPO do exist (20,37), however murine MPO lacks several
111 transcription factor binding domains (38), and is expressed at 1/10 the level found in
112 human neutrophils (39), raising concerns over whether a murine model can fully
113 represent human MPO.

114 In this study, we have generated a transgenic zebrafish line expressing
115 fluorescently-labelled human MPO in zebrafish neutrophils, as a tool towards
116 investigating the roles of MPO during infection and inflammation. The transgene for
117 the MPO-mEmerald fusion protein (*lyz:Hsa.MPO-mEmerald*) was successfully
118 expressed in zebrafish neutrophils and the resulting protein appears to be trafficked
119 to granules, recapitulating expression of MPO in human neutrophils. Additionally, we
120 showed that the MPO-mEmerald enzyme does not disrupt neutrophil recruitment to
121 sites of injury and infection. In the future, *Tg(lyz:Hsa.MPO-*
122 *mEmerald,cmlc2:EGFP)sh496* zebrafish may prove to be a useful tool for
123 investigating MPO and imaging granular dynamics *in vivo* and in real-time.

124 Methods

125

126 **Zebrafish Husbandry**

127 Zebrafish (*Danio rerio*) were raised and maintained under the Animals (Scientific
128 Procedures) Act 1986 using standard protocols (40). Adult zebrafish were hosted in
129 UK Home Office-approved aquaria at the Bateson Centre, University of Sheffield,
130 and kept under a 14/10 light/dark regime at 28°C.

131

132 **Cloning the *Tg(lyz:Hsa.MPO-mEmerald,cm12:EGFP)sh496* line**

133 The plasmid used for introducing the transgene into the zebrafish genome
134 (pDestTol2CG2 *lyz:MPO-mEmerald cm1c2:EGFP*) was created by Gateway cloning
135 (31). Briefly, a gateway vector p5E-MCS containing 6.6kb of the lysozyme C
136 promoter (33) was used to drive neutrophil-specific expression, . The MPO-
137 mEmerald gene was incorporated into an expression vector by first digesting the
138 mEmerald-MPO-N-18 plasmid (Addgene plasmid #54187, Dr. Michael Davidson's
139 lab), and ligating the MPO-mEmerald fusion protein gene into the multiple cloning
140 site vector pME MCS to generate the middle-entry vector, pME MCS MPO-
141 mEmerald. The final construct was created by an LR reaction combining a 5' vector
142 containing the *lyz* promoter, the middle entry vector pME MPO-mEmerald, a 3'
143 vector containing a polyadenylation site, and the destination vector pDestTol2CG2.

144

145 **Generation of the *Tg(lyz:nfsB-mCherry)sh260* line**

146 As for the MPO-mEmerald construct, the *lyz* promoter in the gateway vector p5E-
147 MCS was used to drive neutrophil-specific expression. For red fluorescence,
148 mCherry was produced as a fusion protein with the nitroreductase gene *nfsB*

149 (primers F: 5' GGG GAC AAG TTT GTA CAA AAA AGC AGG CTG CAT GGA TAT
150 CAT TTC TGT CGC CTT, R: 5' GGG GAC CAC TTT GTA CAA GAA AGC TGG
151 GTC GGT CCA CTT CGG TTA AGG TGA TGT T), which also permits conditional
152 ablation of cells upon addition of metronidazole (41), and cloned into middle entry
153 (pME-nfsB) and 3' entry vectors (p3E-mCherry). The final *lyz:nfsB-mCherry*
154 construct was created by recombination of p5E-*lyz*, pME-nfsB, and p3E-mCherry,
155 and pDestTol2pA2.

156

157 **Microinjection of *lyz:MPO-mEmerald* Construct DNA**

158 Construct DNA of the donor plasmid pDestTol2CG2 *lyz:MPO-mEmerald*
159 *cm1c2:EGFP* or pDestTol2pA2 *lyz:nfsB-mCherry* was injected into zebrafish embryos
160 at the one-cell stage with 10ng/μl of Tol2 transposase RNA, according to published
161 protocols (40).

162

163 **TSA staining and colocalisation experiments**

164 3dpf *Tg(lyz:Hsa.MPO-mEmerald,cm1c2:EGFP)sh496* larvae were fixed in ice-cold
165 4% (w/v) paraformaldehyde (PFA) in PBS-TX (PBS supplemented with 0.5 % of
166 Triton X-100) overnight at 4°C. Fixed embryos were washed in PBS-TX twice.
167 Peroxidase activity was detected by incubation in 1:50 Cy5-TSA:amplification
168 reagent (PerkinElmer, Waltham, MA) in the dark for 10 min at 28°C followed by
169 extensive washing in PBS-TX.

170

171 **Zebrafish Tailfin Transection**

172 *Tg(lyz:Hsa.MPO-mEmerald,cm1c2:EGFP)sh496* zebrafish at 3 days post-fertilisation
173 were anaesthetised by immersion in E3 supplemented with 4.2% Tricaine and
174 complete transection of the tail was performed with a sterile scalpel. For imaging of

175 larvae, a Nikon® custom-build wide-field microscope was used: Nikon® Ti-E with a
176 CFI Plan Apochromat λ 10X, N.A.0.45 objective lens, a custom built 500 μ m Piezo Z-
177 stage (Mad City Labs, Madison, WI, USA) and using Intensilight fluorescent
178 illumination with ET/sputtered series fluorescent filters 49002 and 49008 (Chroma,
179 Bellow Falls, VT, USA) was used. Analysis was performed using Nikon's® NIS
180 Elements software package.

181

182 **Bacterial Culture Preparation**

183 To prepare a liquid overnight culture of *S. aureus*, 5ml of BHI broth medium (Oxoid)
184 was inoculated with a colony of *S. aureus* strain USA300, and incubated at 37°C
185 overnight with shaking. To prepare *S. aureus* for injection, 50ml of BHI media was
186 inoculated with 500 μ l of overnight culture and incubated for roughly 2 hours at 37°C
187 with shaking. The OD₆₀₀ of each culture was measured and 40ml of the remaining
188 culture harvested by centrifugation at 4,500g for 15 minutes at 4°C. The pellet was
189 then resuspended in a volume of PBS appropriate to the bacterial dose required.
190 Once the pellets were resuspended they were then kept on ice until required.

191

192 **Spotless (*mpx*^{NL144}) Fish and Sudan Black Staining**

193 The Spotless (*mpx*^{NL144}) mutant line contains a C to T mutation at nucleotide 1126 of
194 the *mpx* RefSeq mRNA sequence (NM_212779), resulting in a premature stop
195 codon (42). A detailed protocol of Sudan Black B staining can be found in
196 Supplementary File 1.

197

198 **Microscopy of Neutrophil Granules**

199 Microscopy of neutrophil granules in *Tg(Iyz:Hsa.MPO-mEmerald,cmlc2:EGFP)sh496*

200 larvae was performed using a Zeiss® Axiovert LSM 880 Airyscan confocal

201 microscope with 63x Plan Apochromat oil objective (NA 1.4). Cells were illuminated

202 with a 488 nm argon laser and/or a 561 nm diode laser. Images were processed

203 using the Zeiss® microscope software and analysed using Zen Black.

204

205 **Statistics**

206 All data were analysed (Prism 7.0, GraphPad Software, San Diego, CA, USA) using

207 a two-way ANOVA with Bonferroni post-test to adjust for multiple comparisons.

208 Results

209

210 **Creation of a transgenic zebrafish expressing human myeloperoxidase**

211 To create a transgenic zebrafish that expresses a fluorescently-tagged human
212 myeloperoxidase (MPO), we created a genetic construct using Gateway cloning that
213 contains the MPO gene with a C-terminal fusion of the fluorescent protein mEmerald,
214 driven by the neutrophil-specific promoter *lyz* (Figure 1A). After the construct was
215 successfully assembled, it was introduced into the zebrafish genome by Tol2-
216 mediated transgenesis. To verify expression in neutrophils, a second transgenic line
217 was created using a construct expressing mCherry under the *lyz* promoter,
218 *Tg(lyz:nfsB-mCherry)sh260*. Successful expression of MPO-mEmerald in zebrafish
219 neutrophils was confirmed by inducing transgenesis in *Tg(lyz:nfsB-mCherry)sh260*
220 fish (Figure 1CD). Injected larvae were then screened at 3 days post fertilisation
221 (dpf) for mEmerald expression and colocalisation with mCherry expression. Figure
222 1CD shows double-transgenic neutrophils expressing both mEmerald and mCherry
223 in the primary haematopoietic tissue of the zebrafish larvae, the caudal
224 haematopoietic tissue (CHT) (indicated in Figure 1B) (43). This observation confirms
225 that the construct is successfully expressed and suggests that it co-localises with
226 zebrafish neutrophils. We also noted that in double-transgenic neutrophils, there
227 appeared to be a differential subcellular localisation between mEmerald and
228 mCherry signal, with mCherry localised to areas with no visible mEmerald signal
229 (Figure 1D).

230

231 **MPO-mEmerald is stably expressed in zebrafish neutrophils**

232 To secure adult zebrafish with stable germline integrations of the *lyz:MPO-mEmerald*
233 transgene, larvae that transiently expressed the transgene were identified, raised
234 and outcrossed to determine whether the transgene was inherited by their offspring.
235 An adult that produced larvae with a cell population labelled with mEmerald was
236 identified and its progeny raised to produce fish stably expressing the MPO
237 transgene, with the designation *Tg(lyz:Hsa.MPO-mEmerald,cm1c2:EGFP)sh496*. To
238 verify whether the *lyz:MPO-mEmerald* transgene was expressed in neutrophils of
239 stably transgenic fish, they were crossed to the red neutrophil reporter line
240 *Tg(lyz:nfsB-mCherry)sh260*, and screened for any co-expression of fluorescent
241 proteins. Both transgenes were expressed in neutrophils throughout the CHT (Figure
242 2), demonstrating that *lyz:MPO-mEmerald* is expressed in zebrafish neutrophils in
243 stably transgenic larvae.

244 To further confirm that MPO-mEmerald positive cells are neutrophils, we
245 performed TSA-staining on fixed larvae at 3dpf (Figure 4), to stain specific
246 endogenous peroxidase activity in zebrafish neutrophils (44). An average of 80% of
247 the cells observed in the CHT are positive for both MPO-mEmerald and TSA,
248 suggesting that the transgene specifically labels neutrophils in the larva – the
249 staining of neutrophils with TSA is incomplete accounting for the less than 100% co-
250 staining.

251

252 **MPO-mEmerald is trafficked to a subcellular location**

253 As MPO is located in the primary granules of neutrophils prior to delivery to the
254 phagosome (1), we wished to determine whether the *lyz:MPO-mEmerald* transgene
255 recapitulates MPO expression in human neutrophils. To investigate the intracellular

256 localisation of the MPO transgene, *Tg(lyz:Hsa.MPO-mEmerald,cmlc2:EGFP)sh496*
257 fish were outcrossed to *Tg(lyz:nfsB-mCherry)sh260* fish, and at 3dpf the double-
258 transgenic larvae were imaged in high detail using an Airyscan confocal microscope.
259 Both transgenes are expressed in the same cells, with MPO-mEmerald localising
260 with a granular subcellular distribution (Figure 3), suggesting that the MPO-
261 mEmerald fusion protein is trafficked to and packaged within neutrophil granules.
262 High-speed imaging of a double-transgenic *Tg(lyz:Hsa.MPO-*
263 *mEmerald,cmlc2:EGFP)sh496; Tg(lyz:nfsB-mCherry)sh260* larva shows that the
264 intracellular MPO-mEmerald signal is highly dynamic (Supplemental movie 1), and
265 resembles the Brownian motion that would be observed in primary neutrophil
266 granules. Additionally, we also analysed colocalisation of the MPO-mEmerald signal
267 with the location of TSA histochemical staining in neutrophils (Figure 5). There was
268 70% colocalisation between MPO-mEmerald and endogenous peroxidase activity
269 (the MPO transgene does not have peroxidase activity – see below). This suggests
270 that MPO-mEmerald is expressed in neutrophil granules, with the differences in co-
271 localisation due to inactive, unprocessed forms of MPO-mEmerald.

272

273 **MPO-mEmerald does not disrupt neutrophil migration**

274 In addition to its role in potentiating ROS generation in neutrophils, MPO also
275 influences neutrophil migration to inflammatory stimuli (16). Accordingly, we sought
276 to determine whether *Tg(lyz:Hsa.MPO-mEmerald,cmlc2:EGFP)sh496* fish exhibit
277 disrupted neutrophil migration to inflammatory and infectious stimuli.
278 *Tg(lyz:Hsa.MPO-mEmerald,cmlc2:EGFP)sh496* fish were crossed to *Tg(lyz:nfsB-*
279 *mCherry)sh260* and at 3dpf their larvae were separated into two groups: non-

280 humanised (*lyz:nfsB-mCherry* only) and humanised (*lyz:MPO-mEmerald*; *lyz:nfsB-*
281 *mCherry*) to determine how expression of MPO-mEmerald affects these responses.

282 To assess neutrophil migration to inflammatory stimuli, we used a tailfin-
283 transection model that initiates neutrophil recruitment to a vertically transected tailfin
284 injury in zebrafish larvae (35). Non-humanised and humanised larvae were injured
285 and neutrophil recruitment to the site of injury was imaged at 3 and 6 hours post
286 injury (hpi) (Figure 6A). Both groups exhibited comparable migration of neutrophils to
287 the site of injury at 3 and 6hpi (Figure 6B), suggesting that *lyz:MPO-mEmerald* does
288 not interfere with neutrophil recruitment to sites of injury.

289 To determine whether the neutrophil response to infection is affected by
290 expression of *lyz:MPO-mEmerald*, we used an otic vesicle infection model to
291 investigate neutrophil recruitment (45,46). After separating larvae into non-
292 humanised and humanised groups, they were injected into the otic vesicle with either
293 a PBS vehicle control or *S. aureus* USA300 at 3dpf. The larvae were then fixed in
294 paraformaldehyde at 4 hours post infection (hpi) and stained with Sudan Black B to
295 detect neutrophils. Injection of *S. aureus* USA300 induces robust recruitment of
296 neutrophils to the otic vesicle, with comparable numbers recruited between non-
297 humanised and humanised larvae (Figure 6CD). This confirms that expression of the
298 *lyz:MPO-mEmerald* transgene does not interfere with neutrophil recruitment to sites
299 of infection.

300

301 **Genotypic and functional identification of myeloperoxidase-null *Spotless***
302 **(*mpx^{NL144}*) larvae**

303 While the *lyz:MPO-mEmerald* transgene is expressed in zebrafish neutrophils in a
304 manner that recapitulates expression in human neutrophils, it was still unknown

305 whether MPO-mEmerald is expressed as a functional enzyme. To determine
306 whether MPO was functional, we sought to create a zebrafish that expresses only
307 human MPO by removing expression of the endogenous zebrafish myeloperoxidase
308 (*mpx*) from the *Tg(lyz:Hsa.MPO-mEmerald,cmlc2:EGFP)sh496* line. This was
309 achieved using an existing zebrafish line known as Spotless (*mpx^{NL144}*), which
310 possesses a premature stop codon in the first exon of the *mpx* gene (42). Once
311 acquired, we aimed to cross the Spotless line to our *Tg(lyz:Hsa.MPO-*
312 *mEmerald,cmlc2:EGFP)sh496* line to create a line that expresses only human MPO.
313 Before we could create this line, it was necessary to develop a genotyping protocol
314 that could accurately identify Spotless *mpx^{NL144}* fish.

315 The *mpx^{NL144}* allele can be identified by PCR amplification of the mutated
316 gene from genomic DNA, followed by restriction digest of the PCR product. The
317 restriction enzyme *BtsCI* recognises 5' GG ATG NN 3' sites in DNA, one of which is
318 present within the mutated *mpx^{NL144}* gene (GGA TGA) but not the wild-type *mpx^{wt}*
319 gene (GGA CGA), allowing the enzyme to determine the presence of a *mpx^{NL144}*
320 allele (Figure 7A). The PCR primers were successful in amplifying the region in the
321 *mpx* gene from *mpx^{wt}*, *mpx^{NL144}* and *mpx^{wt/NL144}* groups (Figure 7B), and once
322 digested with *BtsCI* produced different DNA fragments depending on the *mpx^{NL144}*
323 allele of the fish (Figure 7C), confirming *BtsCI* digestion as an efficient means of
324 identifying the *mpx^{NL144}* allele. The accuracy of the restriction digest was confirmed
325 further by sequencing the PCR products, confirming that the fish identified by
326 restriction digest each have the specific basepair in the expected position (Figure
327 7D). After adults were genotyped, their larvae were then assessed for functional
328 myeloperoxidase expression using the myeloperoxidase-dependent stain Sudan
329 Black B (16) (Supplemental file 1), which verified the genotyping results (Figure 7E).

330

331 **MPO-mEmerald is non-functional in zebrafish neutrophils**

332 To create zebrafish larvae expressing only human MPO, the *Tg(lyz:Hsa.MPO-*
333 *mEmerald,cmlc2:EGFP)sh496* line was crossed to the Spotless line to create
334 zebrafish that express the *lyz:MPO-mEmerald* transgene and do not produce
335 functional endogenous *mpx*. Once created, *Tg(lyz:Hsa.MPO-*
336 *mEmerald,cmlc2:EGFP)sh496; mpx^{NL144}* larvae were stained with the
337 myeloperoxidase-dependent stain Sudan Black B to determine whether this
338 conferred staining; these larvae were compared against three sibling control groups
339 – *mpx^{NL144}*, *mpx^{wt/NL144}* and *Tg(lyz:Hsa.MPO-mEmerald,cmlc2:EGFP)sh496;*
340 *mpx^{wt/NL144}*. All groups tested containing a functioning *mpx* allele (*mpx^{wt/NL144}*,
341 *Tg(lyz:Hsa.MPO-mEmerald,cmlc2:EGFP)sh496; mpx^{wt/NL144}*) stained with Sudan
342 Black B, indicating that the stain identifies functional endogenous myeloperoxidase
343 (Figure 8). As expected, the negative control group did not stain (*mpx^{NL144}*), but
344 surprisingly, neither did the *Tg(lyz:Hsa.MPO-mEmerald,cmlc2:EGFP)sh496;*
345 *mpx^{NL144}* human MPO-only larvae, indicating that the *lyz:MPO-mEmerald* transgene
346 does not produce a functional MPO enzyme (Figure 8).

347 Discussion

348

349 In this study, we created a transgenic line expressing a fluorescently-tagged human
350 myeloperoxidase in zebrafish neutrophils. Expression in neutrophils was determined
351 by observing expression of *lyz:MPO-mEmerald* in the fluorescent red neutrophil line,
352 *Tg(lyz:nfsB-mCherry)sh260*, which expresses mCherry in the cytoplasm of zebrafish
353 neutrophils. Both transgenes were expressed within the same cells (Figure 1, 2), and
354 TSA staining showed that the majority of MPO-mEmerald cells produced active
355 peroxidase that colocalises with MPO-mEmerald signal (Figure 4) confirming that the
356 *lyz:MPO-mEmerald* transgene labels neutrophils. However, as MPO localises with
357 the primary granules of neutrophils, it was essential that the fluorescent signal
358 observed in the *lyz:MPO-mEmerald* line should differ from the cytoplasmic signal
359 observed in the *Tg(lyz:nfsB-mCherry)sh260* line. This was observed in several
360 instances; in double transgenic neutrophils, distinct areas of the cell remain
361 unlabelled with mEmerald (Figures 1, 3) suggesting that MPO is translated and
362 trafficked to a subcellular location that is distinct from the cytoplasm. This
363 observation is also evident in Airyscan confocal imaging (Figure 3C), where a large
364 unlabelled area of a double-transgenic neutrophil is visible in the mEmerald channel.
365 This is likely to be a region of the cell that is inaccessible to the primary granules, for
366 example the nucleus, and could be verified using a fluorescent nuclear probe.

367 In addition to the *lyz:MPO-mEmerald* and *lyz:nfsB-mCherry* signals being
368 distinct, double-transgenic neutrophils contain small intracellular foci of mEmerald
369 signal (Figure 3), suggesting that MPO-mEmerald might be targeted to the primary
370 granules. Using high-speed imaging, we found that these foci are highly dynamic,
371 resembling the Brownian motion exhibited by neutrophil granules (Supplemental

372 movie 1). Despite these observations, we found that an average of 80% of cells
373 expressing MPO-mEmerald stain with peroxidase-sensitive TSA, and 70% of
374 mEmerald signal colocalises with TSA signal (Figure 5). It is important to note that
375 not all labelled MPO would localise with active peroxidase, as immature MPO
376 present in the endoplasmic reticulum and trans-golgi network prior to dimerisation
377 would also be visible in MPO-mEmerald fish (47). Additionally, it is likely that
378 neutrophils at different stages of development would contain different levels of
379 functional MPO, which may explain incomplete staining with TSA.

380 In addition to the role of MPO in antibacterial defence, it is also an important
381 enzyme regulating the migration of neutrophils to sites of infection and inflammation,
382 primarily by mediating H₂O₂ flux (16). Using a combination of approaches for
383 studying neutrophil migration, we found that expression of the *lyz:MPO-mEmerald*
384 transgene does not interfere with neutrophil recruitment to sites of infection and
385 inflammation (Figure 6). Currently, there are no existing tools for visualising
386 neutrophil granules *in vivo*, and measuring MPO is limited to cytochemical and
387 cytometry-based approaches (36). Therefore, the *Tg(lyz:Hsa.MPO-*
388 *mEmerald,cmlc2:EGFP)sh496* transgenic line may be used to study granule
389 dynamics *in vivo* without disrupting neutrophil function.

390 In order to determine whether MPO-mEmerald is produced as a functional
391 enzyme, it was necessary to produce zebrafish that do not express endogenous
392 zebrafish myeloperoxidase. We describe here a genotyping protocol that can be
393 used to identify Spotless (*mpx^{NL144}*) fish, an *mpx*-null mutant line created in a
394 separate study (42). This was accomplished by amplifying a region present in the
395 first exon of the *mpx* gene, followed by restriction digest with *BtsCI* (Figure 7BCD);
396 this was then functionally verified using the myeloperoxidase-dependent stain Sudan

397 Black B (16) (Figure 7E). We believe this to be a useful and robust method for
398 identifying Spotless fish, and may be useful in future studies.

399 Once a robust method for identifying Spotless fish was established, the
400 Spotless line was crossed to the *Tg(lyz:Hsa.MPO-mEmerald,cmlc2:EGFP)sh496* line
401 to generate a line that expresses human MPO, and does not express zebrafish Mpx
402 (known as *Tg(lyz:Hsa.MPO-mEmerald,cmlc2:EGFP)sh496; mpx^{NL144}*). By comparing
403 staining with Sudan Black B with sibling controls, we found that MPO-mEmerald is
404 not produced as a functional enzyme, as *lyz:MPO-mEmerald* expression does not
405 complement staining in the *mpx^{NL144}* background. It is unclear why the
406 *Tg(lyz:Hsa.MPO-mEmerald,cmlc2:EGFP)sh496* line does not produce functional
407 MPO, however it is important to note that MPO is a complex glycoprotein enzyme
408 that undergoes numerous tightly regulated post-translational modifications. Before
409 mature MPO is produced, the peptide associates with calreticulin and calnexin in the
410 endoplasmic reticulum before undergoing a series of proteolytic events leading to
411 insertion of a haem group and dimerisation of the enzyme, followed by glycosylation
412 and ending with granule targeting (47). The importance of each step in producing a
413 functional enzyme is unclear, however studies of myeloperoxidase-deficient
414 individuals suggest that targeting to the primary granules universally correlates with
415 functional MPO (23,48–50), and *in vitro* studies show that dimerisation is not
416 required for enzyme function (15,51,52). Additionally, the discrepancy is unlikely to
417 lie with calnexin and calreticulin, as they possess roughly 70% amino acid identity
418 with the human chaperones, and are important during development of the zebrafish
419 lateral line (53). Differences at any other stages may lead to incomplete MPO
420 maturation and function in the zebrafish and consequently, the *Tg(lyz:Hsa.MPO-*

421 *mEmerald,cmlc2:EGFP)sh496* line may also be useful in investigating how MPO is
422 processed and targeted to the granules during development.

423

424 Conclusion

425

426 We have generated a transgenic zebrafish line expressing fluorescently labelled
427 human MPO within its neutrophils. The enzyme is non-functional and does not
428 interfere with neutrophil recruitment to sites of infection or inflammation, suggesting
429 that it may be used to study granule dynamics *in vivo* without disrupting neutrophil
430 behaviour. Additionally, the *Tg(lyz:Hsa.MPO-mEmerald,cmlc2:EGFP)sh496* line may
431 be used to investigate processing and targeting of MPO during development, which
432 is currently uncharacterised *in vivo*. Lastly, we provide a protocol for genotyping
433 endogenous myeloperoxidase-null Spotless (*mpx^{NL144}*) fish, which will prove useful in
434 future studies investigating myeloperoxidase in the zebrafish.

435 References

436

- 437 1. Klebanoff SJ, Kettle a. J, Rosen H, Winterbourn CC, Nauseef WM.
438 Myeloperoxidase: a front-line defender against phagocytosed microorganisms.
439 Vol. 93, Journal of Leukocyte Biology. 2012. p. 185–98.
- 440 2. Kettle AJ, Winterbourn CC. Myeloperoxidase: a key regulator of neutrophil
441 oxidant production. Redox Rep. 1997 Feb 13;3(1):3–15.
- 442 3. Borregaard N, Cowland JB. Granules of the human neutrophilic
443 polymorphonuclear leukocyte. Blood. 1997 May 15;89(10):3503–21.
- 444 4. Decleva E, Menegazzi R, Busetto S, Patriarca P, Dri P. Common methodology
445 is inadequate for studies on the microbicidal activity of neutrophils. J Leukoc
446 Biol. 2006;79(1):87–94.
- 447 5. Aratani Y, Kura F, Watanabe H, Akagawa H, Takano Y, Suzuki K, et al. Critical
448 Role of Myeloperoxidase and Nicotinamide Adenine Dinucleotide Phosphate –
449 Oxidase in High-Burden Systemic Infection of Mice with *Candida albicans*. J
450 Infect Dis. 2002;(April):1833–7.
- 451 6. Hirche TO, Gaut JP, Heinecke JW, Belaouaj A. Myeloperoxidase plays
452 critical roles in killing *Klebsiella pneumoniae* and inactivating neutrophil
453 elastase: effects on host defense. J Immunol. 2005 Feb 1;174(3):1557–65.
- 454 7. Levine AP, Duchon MR, de Villiers S, Rich PR, Segal AW. Alkalinity of
455 Neutrophil Phagocytic Vacuoles Is Modulated by HVCN1 and Has
456 Consequences for Myeloperoxidase Activity. PLoS One. 2015 Apr
457 17;10(4):e0125906.
- 458 8. Reeves EP, Lu H, Jacobs HL, Messina CGM, Bolsover S, Gabella G, et al.
459 Killing activity of neutrophils is mediated through activation of proteases by K⁺
460 flux. Nature. 2002 Mar 21;416(6878):291–7.
- 461 9. Urban CF, Reichard U, Brinkmann V, Zychlinsky A. Neutrophil extracellular
462 traps capture and kill *Candida albicans* yeast and hyphal forms. Cell Microbiol.
463 2006 Apr;8(4):668–76.
- 464 10. Thurlow LR, Hanke ML, Fritz T, Angle A, Aldrich A, Williams SH, et al.
465 Staphylococcus aureus biofilms prevent macrophage phagocytosis and
466 attenuate inflammation in vivo. J Immunol. 2011 Jun 1;186(11):6585–96.

- 467 11. Feldmesser M. Role of neutrophils in invasive aspergillosis. *Infect Immun.*
468 2006 Dec 1;74(12):6514–6.
- 469 12. Lardner A. The effects of extracellular pH on immune function. *J Leukoc Biol.*
470 2001 Apr;69(4):522–30.
- 471 13. Papayannopoulos V, Metzler KD, Hakkim A, Zychlinsky A. Neutrophil elastase
472 and myeloperoxidase regulate the formation of neutrophil extracellular traps. *J*
473 *Cell Biol.* 2010 Nov 1;191(3):677–91.
- 474 14. Branzk N, Lubojemska A, Hardison SE, Wang Q, Gutierrez MG, Brown GD, et
475 al. Neutrophils sense microbe size and selectively release neutrophil
476 extracellular traps in response to large pathogens. *Nat Immunol.* 2014
477 Nov;15(11):1017–25.
- 478 15. de Jong NWM, Ramyar KX, Guerra FE, Nijland R, Fevre C, Voyich JM, et al.
479 Immune evasion by a staphylococcal inhibitor of myeloperoxidase. *Proc Natl*
480 *Acad Sci.* 2017 Aug 29;114(35):9439–44.
- 481 16. Pase L, Layton JE, Wittmann C, Ellett F, Nowell CJ, Reyes-Aldasoro CC, et al.
482 Neutrophil-delivered myeloperoxidase dampens the hydrogen peroxide burst
483 after tissue wounding in zebrafish. *Curr Biol.* 2012;22(19):1818–24.
- 484 17. Schürmann N, Forrer P, Casse O, Li J, Felmy B, Burgener A, et al.
485 Myeloperoxidase targets oxidative host attacks to *Salmonella* and prevents
486 collateral tissue damage. *Nat Microbiol.* 2017 Jan 23;2(January):16268.
- 487 18. Kutter D, Devaquet P, Vanderstocken G, Paulus JM, Marchal V, Gothot A.
488 Consequences of Total and Subtotal Myeloperoxidase Deficiency: Risk or
489 Benefit? *Acta Haematol.* 2000;104(1):10–5.
- 490 19. Yang JJ, Pendergraft WF, Alcorta DA, Nachman PH, Hogan SL, Thomas RP,
491 et al. Circumvention of normal constraints on granule protein gene expression
492 in peripheral blood neutrophils and monocytes of patients with antineutrophil
493 cytoplasmic autoantibody-associated glomerulonephritis. *J Am Soc Nephrol.*
494 2004 Aug 1;15(8):2103–14.
- 495 20. Chen JW, Breckwoldt MO, Aikawa E, Chiang G, Weissleder R.
496 Myeloperoxidase-targeted imaging of active inflammatory lesions in murine
497 experimental autoimmune encephalomyelitis. *Brain.* 2008;131(4):1123–33.
- 498 21. Brennan M-L, Anderson MM, Shih DM, Qu X-D, Wang X, Mehta AC, et al.
499 Increased atherosclerosis in myeloperoxidase-deficient mice. *J Clin Invest.*

- 500 2001 Feb 15;107(4):419–30.
- 501 22. Shvedova AA, Kapralov AA, Feng WH, Kisin ER, Murray AR, Mercer RR, et al.
502 Impaired clearance and enhanced pulmonary inflammatory/fibrotic response to
503 carbon nanotubes in myeloperoxidase-deficient mice. *PLoS One*. 2012 Mar
504 30;7(3):e30923.
- 505 23. DeLeo FR, Goedken M, McCormick SJ, Nauseef WM. A novel form of
506 hereditary myeloperoxidase deficiency linked to endoplasmic
507 reticulum/proteasome degradation. *J Clin Invest*. 1998 Jun 15;101(12):2900–9.
- 508 24. Lehrer RI, Cline MJ. Leukocyte myeloperoxidase deficiency and disseminated
509 candidiasis: the role of myeloperoxidase in resistance to *Candida* infection. *J*
510 *Clin Invest*. 1969;48(8):1478–88.
- 511 25. Magnani A, Brosselin P, Beauté J, de Vergnes N, Mouy R, Debré M, et al.
512 Inflammatory manifestations in a single-center cohort of patients with chronic
513 granulomatous disease. *J Allergy Clin Immunol*. 2014 Sep;134(3):655–662.e8.
- 514 26. Levine AP, Segal AW. The NADPH Oxidase and Microbial Killing by
515 Neutrophils, With a Particular Emphasis on the Proposed Antimicrobial Role of
516 Myeloperoxidase within the Phagocytic Vacuole. *Microbiol Spectr*. 2016 Aug
517 18;4(4):1557–64.
- 518 27. Assari T. Chronic Granulomatous Disease; fundamental stages in our
519 understanding of CGD. *Med Immunol*. 2006;5:4.
- 520 28. Paquet D, Bhat R, Sydow A, Mandelkow E-M, Berg S, Hellberg S, et al. A
521 zebrafish model of tauopathy allows in vivo imaging of neuronal cell death and
522 drug evaluation. *J Clin Invest*. 2009 May;119(5):1382–95.
- 523 29. Haldi M, Ton C, Seng WL, McGrath P. Human melanoma cells transplanted
524 into zebrafish proliferate, migrate, produce melanin, form masses and
525 stimulate angiogenesis in zebrafish. *Angiogenesis*. 2006;9(3):139–51.
- 526 30. Langenau DM, Traver D, Ferrando AA, Kutok JL, Aster JC, Kanki JP, et al.
527 Myc-induced T cell leukemia in transgenic zebrafish. *Science*. 2003 Feb
528 7;299(5608):887–90.
- 529 31. Kwan KM, Fujimoto E, Grabher C, Mangum BD, Hardy ME, Campbell DS, et
530 al. The Tol2kit: A multisite gateway-based construction Kit for Tol2 transposon
531 transgenesis constructs. *Dev Dyn*. 2007 Nov;236(11):3088–99.

- 532 32. Ellett F, Pase L, Hayman JW, Andrianopoulos A, Lieschke GJ. mpeg1
533 promoter transgenes direct macrophage-lineage expression in zebrafish.
534 *Blood*. 2011 Jan 27;117(4):e49-56.
- 535 33. Hall C, Flores MV, Storm T, Crosier K, Crosier P. The zebrafish lysozyme C
536 promoter drives myeloid-specific expression in transgenic fish. *BMC Dev Biol*.
537 2007 May 4;7(1):42.
- 538 34. Elks PM, Brizee S, van der Vaart M, Walmsley SR, van Eeden FJ, Renshaw S
539 a, et al. Hypoxia inducible factor signaling modulates susceptibility to
540 mycobacterial infection via a nitric oxide dependent mechanism. *PLoS Pathog*.
541 2013 Jan;9(12):e1003789.
- 542 35. Renshaw SA, Loynes CA, Trushell DMI, Elworthy S, Ingham PW, Whyte MKB.
543 A transgenic zebrafish model of neutrophilic inflammation. *Blood*. 2006 Dec
544 15;108(13):3976–8.
- 545 36. Pulli B, Ali M, Forghani R, Schob S, Hsieh KLC, Wojtkiewicz G, et al.
546 Measuring myeloperoxidase activity in biological samples. *PLoS One*. 2013 Jul
547 5;8(7):e67976.
- 548 37. Kikushima K, Kita S, Higuchi H. A non-invasive imaging for the in vivo tracking
549 of high-speed vesicle transport in mouse neutrophils. *Sci Rep*. 2013 Dec
550 31;3(1):1913.
- 551 38. Nauseef WM. The proper study of mankind. *J Clin Invest*. 2001 Feb
552 3;107(4):401–3.
- 553 39. Rausch PG, Moore TG. Granule enzymes of polymorphonuclear neutrophils: A
554 phylogenetic comparison. *Blood*. 1975 Dec;46(6):913–9.
- 555 40. Nüsslein-Volhard C, Dahm R. *Zebrafish: A Practical Approach*. Practical.
556 Oxford; New York: Oxford University Press, c2002.; 2002.
- 557 41. Okuda KS, Misa JP, Oehlers SH, Hall CJ, Ellett F, Alasmari S, et al. A
558 zebrafish model of inflammatory lymphangiogenesis. *Biol Open*. 2015 Oct
559 15;4(10):1270–80.
- 560 42. Elks PM, van der Vaart M, van Hensbergen V, Schutz E, Redd MJ, Murayama
561 E, et al. Mycobacteria counteract a TLR-mediated nitrosative defense
562 mechanism in a zebrafish infection model. *PLoS One*. 2014 Jun
563 26;9(6):e100928.

- 564 43. Murayama E, Kissa K, Zapata A, Mordelet E, Briolat V, Lin H-F, et al. Tracing
565 Hematopoietic Precursor Migration to Successive Hematopoietic Organs
566 during Zebrafish Development. *Immunity*. 2006 Dec;25(6):963–75.
- 567 44. Robertson AL, Holmes GR, Bojarczuk AN, Burgon J, Loynes CA, Chimen M,
568 et al. A Zebrafish Compound Screen Reveals Modulation of Neutrophil
569 Reverse Migration as an Anti-Inflammatory Mechanism. *Sci Transl Med*. 2014
570 Feb 26;6(225):225ra29-225ra29.
- 571 45. Benard EL, van der Sar AM, Ellett F, Lieschke GJ, Spaik HP, Meijer AH.
572 Infection of zebrafish embryos with intracellular bacterial pathogens. *J Vis Exp*.
573 2012 Mar 15;(61):1–8.
- 574 46. Deng Q, Sarris M, Bennin D a, Green JM, Herbomel P, Huttenlocher A.
575 Localized bacterial infection induces systemic activation of neutrophils through
576 Cxcr2 signaling in zebrafish. *J Leukoc Biol*. 2013 May;93(5):761–9.
- 577 47. Hansson M, Olsson I, Nauseef WM. Biosynthesis, processing, and sorting of
578 human myeloperoxidase. *Arch Biochem Biophys*. 2006 Jan 15;445(2):214–24.
- 579 48. Nauseef WM. Lessons from MPO deficiency about functionally important
580 structural features. *Jpn J Infect Dis*. 2004;57(5):4–5.
- 581 49. Nauseef WM, Cogley M, McCormick S. Effect of the R569W missense
582 mutation on the biosynthesis of myeloperoxidase. *J Biol Chem*.
583 1996;271(16):9546–9.
- 584 50. Nauseef WM, McCormick S, Goedken M. Impact of missense mutations on
585 biosynthesis of myeloperoxidase. *Redox Rep*. 2000;5(4):197–206.
- 586 51. Moguevsky N, Garcia-Quintana L, Jacquet A, Tournay C, Fabry L, Piérard L,
587 et al. Structural and biological properties of human recombinant
588 myeloperoxidase produced by Chinese hamster ovary cell lines. *Eur J*
589 *Biochem*. 1991 May 8;197(3):605–14.
- 590 52. Andrews PC, Krinsky NI. The reductive cleavage of myeloperoxidase in half,
591 producing enzymically active hemi-myeloperoxidase. *J Biol Chem*. 1981 May
592 10;256(9):4211–8.
- 593 53. Hung I-C, Cherng B-W, Hsu W-M, Lee S-J. Calnexin is required for zebrafish
594 posterior lateral line development. *Int J Dev Biol*. 2013;57(5):427–38.
- 595

596 Acknowledgements

597

598 K.D.B performed experiments with assistance from T.K.P, M.v.G, N.W.M.d.J, and
599 J.K. S.A.R, J.A.G.v.S and S.J.F conceived the study and designed experiments.
600 T.K.P performed TSA-staining and colocalisation experiments. K.D.B and S.A.R
601 wrote the manuscript with significant input from all authors. Thank you to Annemarie
602 Meijer for providing the Spotless (*mpx^{NL144}*) line, to the Bateson Centre aquarium
603 staff for all their help, and to the Wolfson Light Microscopy Facility.

604

605 Conflicts of Interest

606

607 The authors declare no conflicts of interest.

608

609 Funding Information

610

611 This work was supported in part by AMR cross-council funding from the MRC to the
612 SHIELD consortium “Optimising Innate Host Defence to Combat Antimicrobial
613 Resistance” MRNO2995X/1. Microscopy studies were supported by a Wellcome
614 Trust grant to the Molecular Biology and Biotechnology/Biomedical Science Light
615 Microscopy Facility (GR077544AIA).

616 Figure 1. Transient expression of the *lyz*:MPO-mEmerald transgene labels

617 zebrafish neutrophils

618 **A)** Schematic of the *lyz*:MPO-mEmerald *cmlc2*:EGFP construct, which includes the
619 neutrophil-specific promoter (*lyz*), the MPO gene with a C-terminal fluorescent tag
620 (MPO-mEmerald) and a green heart marker to aid optimisation of transgenesis
621 (*cmlc2*:EGFP). **B)** A zebrafish larva at 3 days post fertilisation (dpf), with the caudal
622 haematopoietic tissue (CHT) indicated by the red box. **C)** The CHT of a double-
623 transgenic *Transient lyz*:MPO-mEmerald,*cmlc2*:EGFP; *Tg(lyz:nfsB-mCherry)sh260*
624 larva with a population of neutrophils expressing both mEmerald and mCherry. The
625 white arrowhead indicates the neutrophil enlarged below. **D)** Enlarged view of a
626 neutrophil expressing mEmerald and mCherry.

627 Figure 2. Transgenic *Tg(lyz:Hsa.MPO-mEmerald,cmlc2:EGFP)sh496*

628 zebrafish stably express the transgene in zebrafish neutrophils

629 **A)** A brightfield view of a double-transgenic *Tg(lyz:Hsa.MPO-*
630 *mEmerald,cmlc2:EGFP)sh496; Tg(lyz:nfsB-mCherry)sh260* zebrafish larva at 3dpf.
631 The dashed white box indicates the enlarged region shown in B). **B)** mEmerald and
632 mCherry expression in the CHT of the larva shown in A).

633 Figure 3. The *lyz*:MPO-mEmerald transgene labels intracellular neutrophil

634 granules

635 **A)** 3dpf zebrafish larva, the field of view shown in B) is outlined by the red box. **B)** An
636 Airyscanner confocal image of neutrophils within the CHT of a double-transgenic
637 *Tg(lyz:Hsa.MPO-mEmerald,cmlc2:EGFP)sh496; Tg(lyz:nfsB-mCherry)sh260* larva at
638 3dpf. **C)** An enlarged image of the neutrophil highlighted by the dashed white box in
639 B). Scale bars **B)** 20µm and **C)** 5µm.

640 Figure 4. Most MPO-mEmerald-positive neutrophils are TSA-positive

641 **A)** Confocal photomicrographs shown as maximum intensity projections of *lyz*:MPO-
642 mEmerald larvae fixed at 3 dpf and chemically stained with TSA-Cy5. Dual-positive
643 **(C)** and mEmerald-positive only **(D)** cells are indicated; scale bar 10 μ m. **B)**
644 Quantification of dual positive, TSA-positive only and mEmerald-positive only cells
645 observed in *lyz*:MPO-mEmerald larvae fixed at 3 dpf and chemically stained with
646 TSA-Cy5. Red points indicate larva shown in A).

647 Figure 5. mEmerald signal colocalises with TSA signal

648 **A)** Representative photomicrograph shown as single focal plane of *lyz*:MPO-
649 mEmerald (Green) larvae fixed at 3 dpf and chemically stained with TSA-Cy5 (Red).
650 Scale bar 10 μ m. **B)** Pseudocoloured (heat) images of Red and Green channels and
651 image of colocalised pixels above threshold. **C)** Scatter plot of channel 1 (Red) vs.
652 channel 2 (Green) of the image shown in A and B. The regression line is plotted
653 along with the threshold level for channel 1 (vertical line)
654 and channel 2 (horizontal line). **D)** Pearson's correlation coefficient for the entire
655 image (R_{total}) or for the pixels above thresholds (R_{coloc}) of 3 tested field of views.
656 Mean \pm SEM are indicated in red.

657 Figure 6. Transgene expression does not disrupt neutrophil recruitment to
658 sites of injury or infection

659 **A)** Non-humanised (*lyz*:nfsB-mCherry only) and humanised (*lyz*:MPO-mEmerald;
660 *lyz*:nfsB-mCherry) 3dpf larvae with tailfins transected to induce neutrophil
661 recruitment; dashed outline represents the area in which neutrophils were counted.
662 Scale bar = 250 μ m. **B)** Neutrophils present at the site of injury at 3 and 6 hours post
663 injury (hpi); blue points denote the representative images in A). Error bars shown are
664 mean \pm SEM (n=45 over three independent experiments); groups were analysed

665 using an ordinary two-way ANOVA and adjusted using Bonferroni's multiple
666 comparisons test; ns, $p > 0.9999$. **C)** Non-humanised and humanised larvae injected
667 with either a PBS vehicle control or 1,400cfu *S. aureus* USA300 into the otic vesicle
668 at 3dpf, then fixed in paraformaldehyde at 4 hours post infection (hpi) and stained
669 with Sudan Black B to detect neutrophils; dashed white outline indicates the otic
670 vesicle. **D)** Neutrophils present at the otic vesicle at 4hpi. Scale bars = 250 μ m. Error
671 bars shown are mean \pm SEM (n=25 over two independent experiments); groups
672 were analysed using an ordinary two-way ANOVA and adjusted using Bonferroni's
673 multiple comparisons test. ****, $p < 0.0001$; ns, $p > 0.9999$.

674 Figure 7. Genotyping and verifying *mpx*-null zebrafish larvae

675 **A)** Diagram of a WT (*mpx*^{wt}) and mutated (*mpx*^{NL144}) gene, showing the *Bts*CI
676 restriction site cutting only the mutated *mpx*^{NL144} gene. **B)** PCR amplification of the
677 *mpx* gene from the genomic DNA of *mpx*^{wt}, *mpx*^{wt/NL144} and *mpx*^{NL144} fish – fragment
678 312bp; control DNA is a positive control from a separate genotyping experiment.
679 Hyperladder 1kb. **C)** Diagnostic digest of the PCR product from *mpx*^{wt}, *mpx*^{wt/NL144}
680 and *mpx*^{NL144} fish. Band sizes: *mpx*^{wt}- 312bp, *mpx*^{NL144}- 230bp, *mpx*^{wt/NL144}- 312bp
681 and 230bp. Hyperladder 100bp plus. **D)** DNA sequencing of the PCR products to
682 confirm the accuracy of the *Bts*CI digest. **E)** *mpx*^{wt}, *mpx*^{NL144} and *mpx*^{wt/NL144} larvae
683 fixed at 4dpf and stained with Sudan Black B. Larvae with at least one functional
684 *mpx* allele stained (57/58 *mpx*^{wt}, 20/20 *mpx*^{wt/NL144}) and larvae that do not produce
685 Mpx did not stain (32/32 *mpx*^{NL144}). Inset shows an enlarged view of the region
686 indicated by the dashed white box. Scale bar = 200 μ m.

687 Figure 8. Larvae expressing only human MPO do not stain with
688 myeloperoxidase-dependent Sudan Black B

689 Four groups of larvae were fixed at 4dpf and stained with Sudan Black B: $mpx^{wt/NL144}$,
690 $Tg(lyz:Hsa.MPO-mEmerald,cmlc2:EGFP)sh496$; $mpx^{wt/NL144}$, mpx^{NL144} and
691 $Tg(lyz:Hsa.MPO-mEmerald,cmlc2:EGFP)sh496$; mpx^{NL144} . $mpx^{wt/NL144}$ and
692 $Tg(lyz:Hsa.MPO-mEmerald,cmlc2:EGFP)sh496$; $mpx^{wt/NL144}$ stained (18/18, 16/16
693 respectively); mpx^{NL144} and $Tg(lyz:Hsa.MPO-mEmerald,cmlc2:EGFP)sh496$;
694 mpx^{NL144} did not stain (20/20, 22/22 respectively). Dashed outline indicates the
695 enlarged region shown adjacent. Scale bar = 200 μ m.

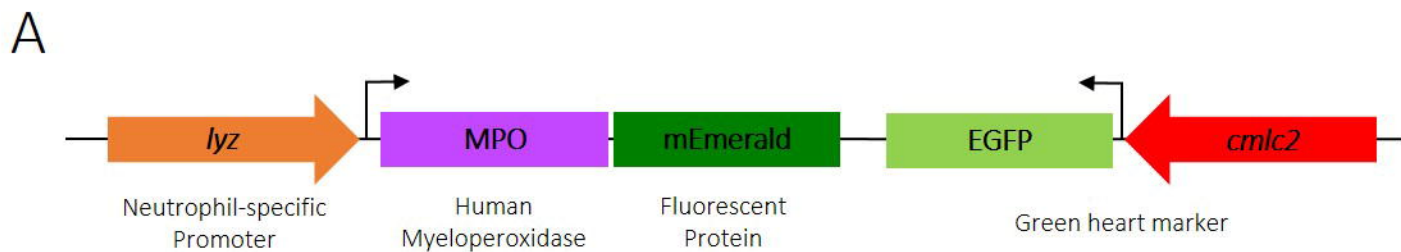
696

697 Supplemental movie 1. MPO-mEmerald signal is highly dynamic

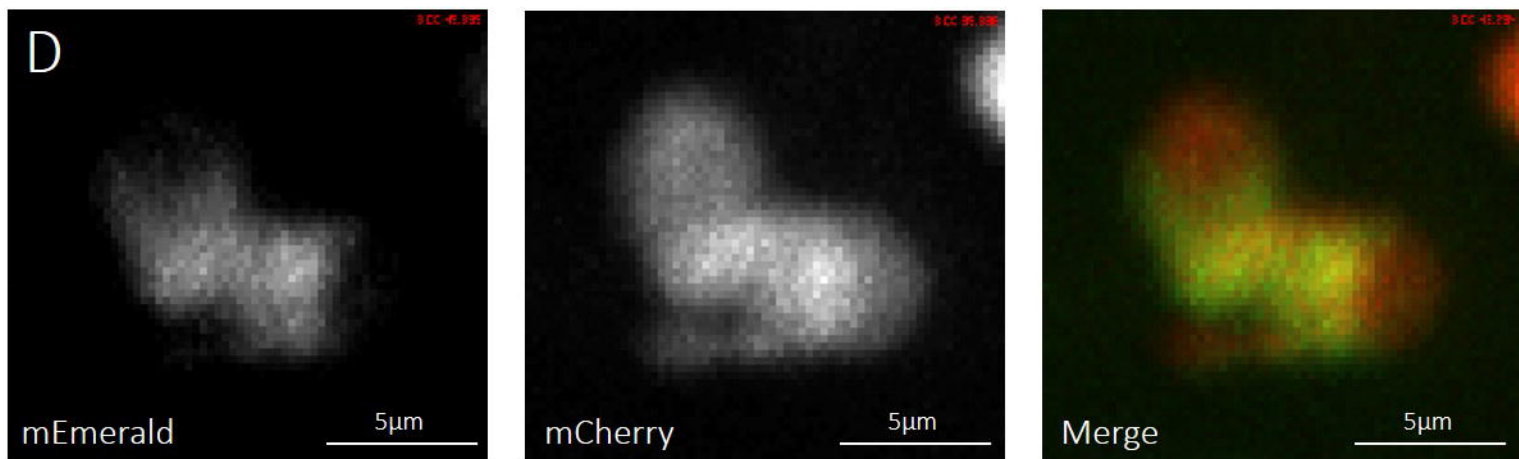
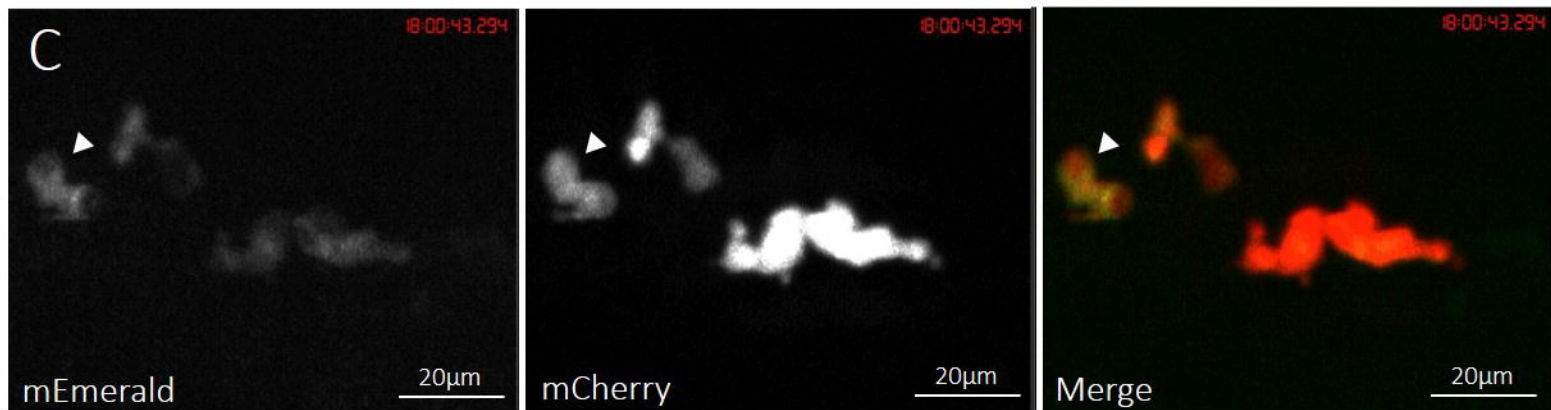
698 An airyscanner confocal timelapse of a double-transgenic $Tg(lyz:Hsa.MPO-$
699 $mEmerald,cmlc2:EGFP)sh496$; $Tg(lyz:nfsB-mCherry)sh260$ larva. The timelapse
700 shows numerous neutrophils in the caudal haematopoietic tissue of a 3dpf larva.

701

702 Supplemental file 1. Sudan Black B Staining Protocol

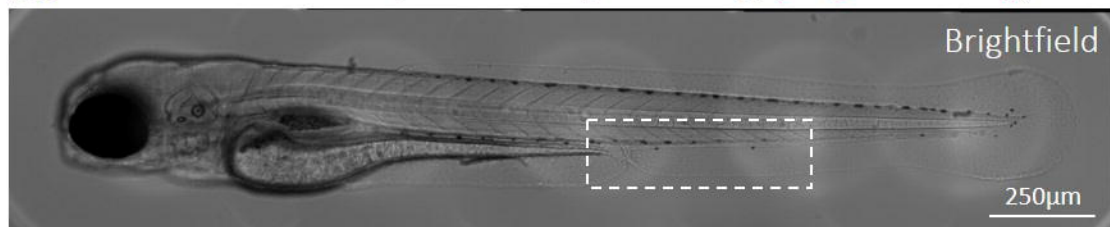


Transient *lyz:Hsa.MPO-mEmerald,cmlc2:EGFP* / *Tg(lyz:nfsB-mCherry)sh260*

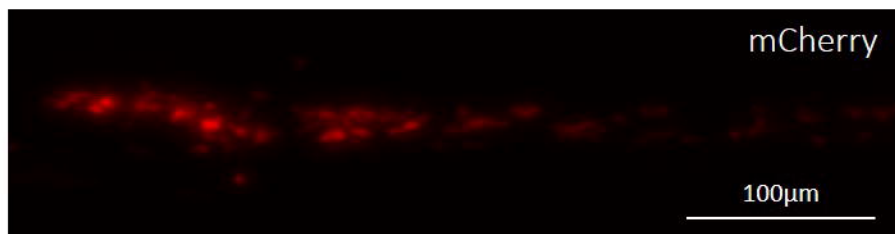
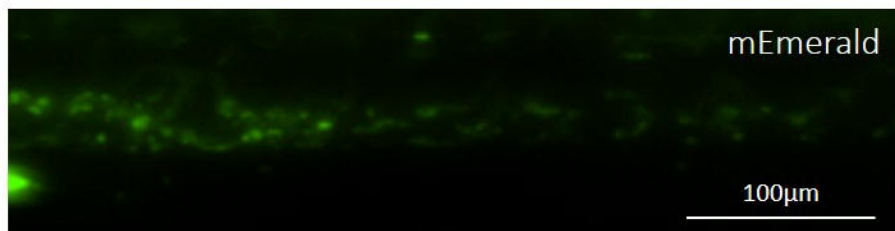


A

Tg(lyz:Hsa.MPO-mEmerald,cmlc2:EGFP)sh496 x *Tg(lyz:nfsB-mCherry)sh260*



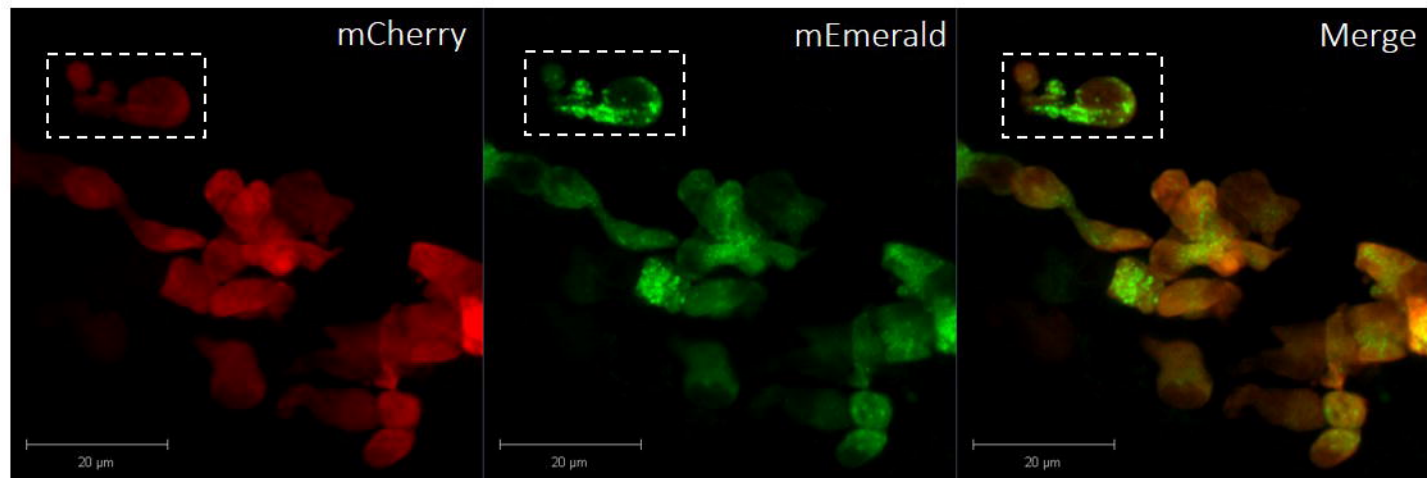
B



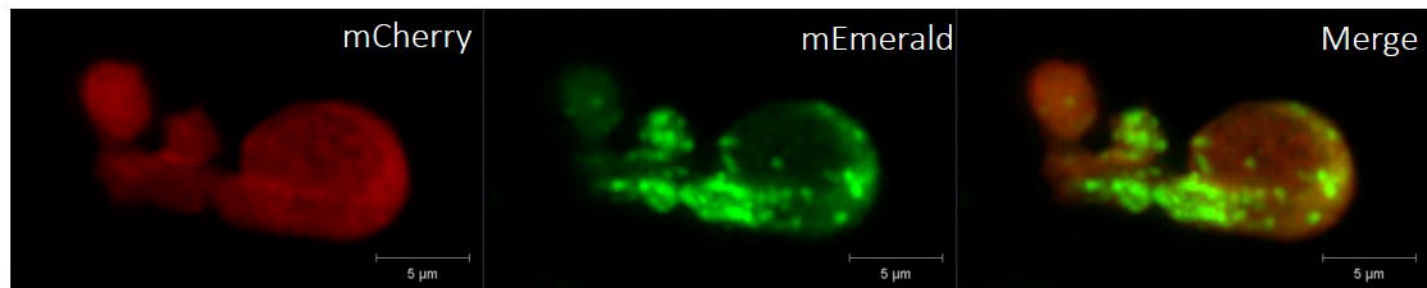
A

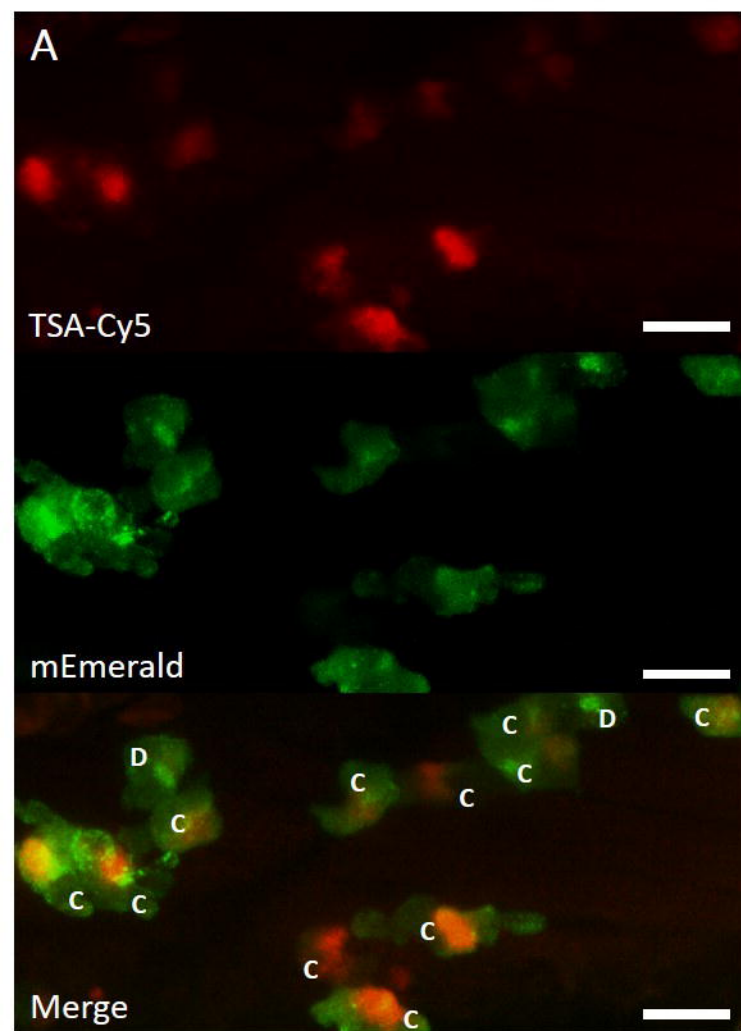


B

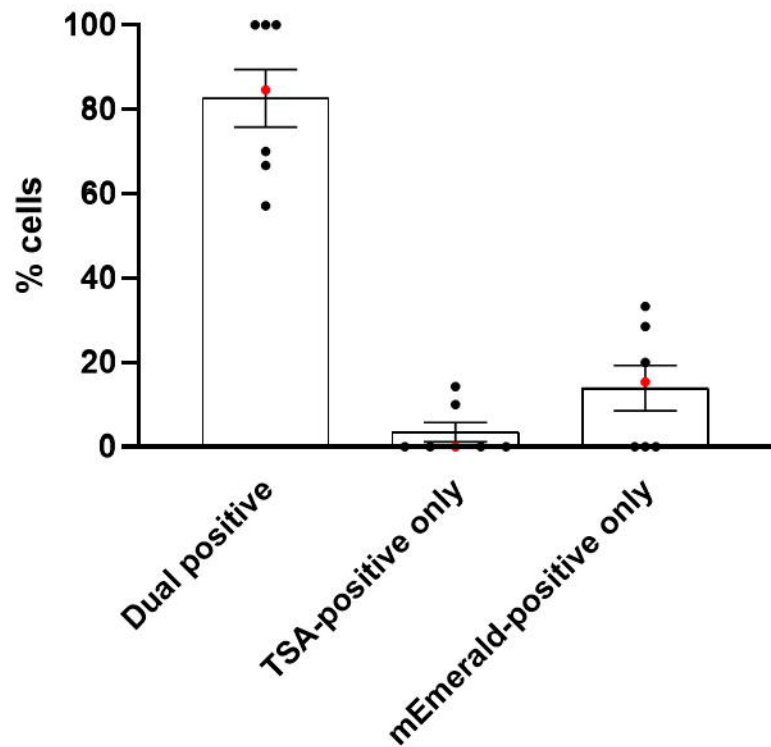


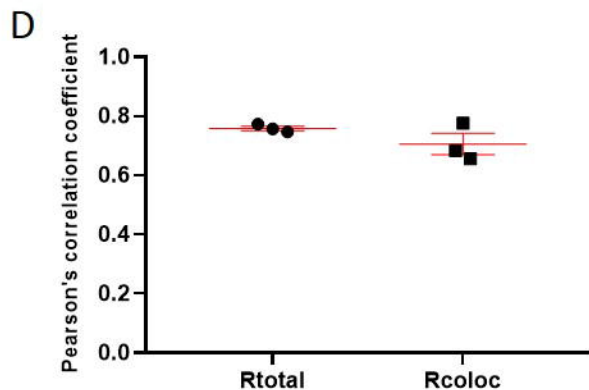
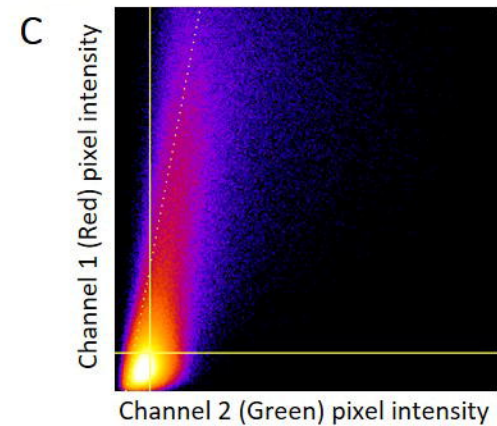
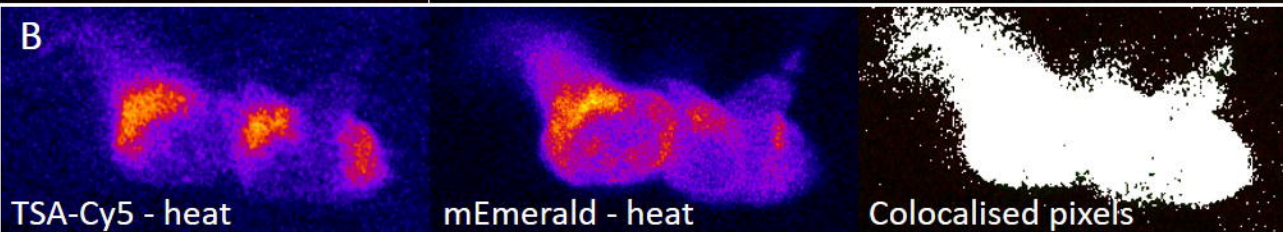
C



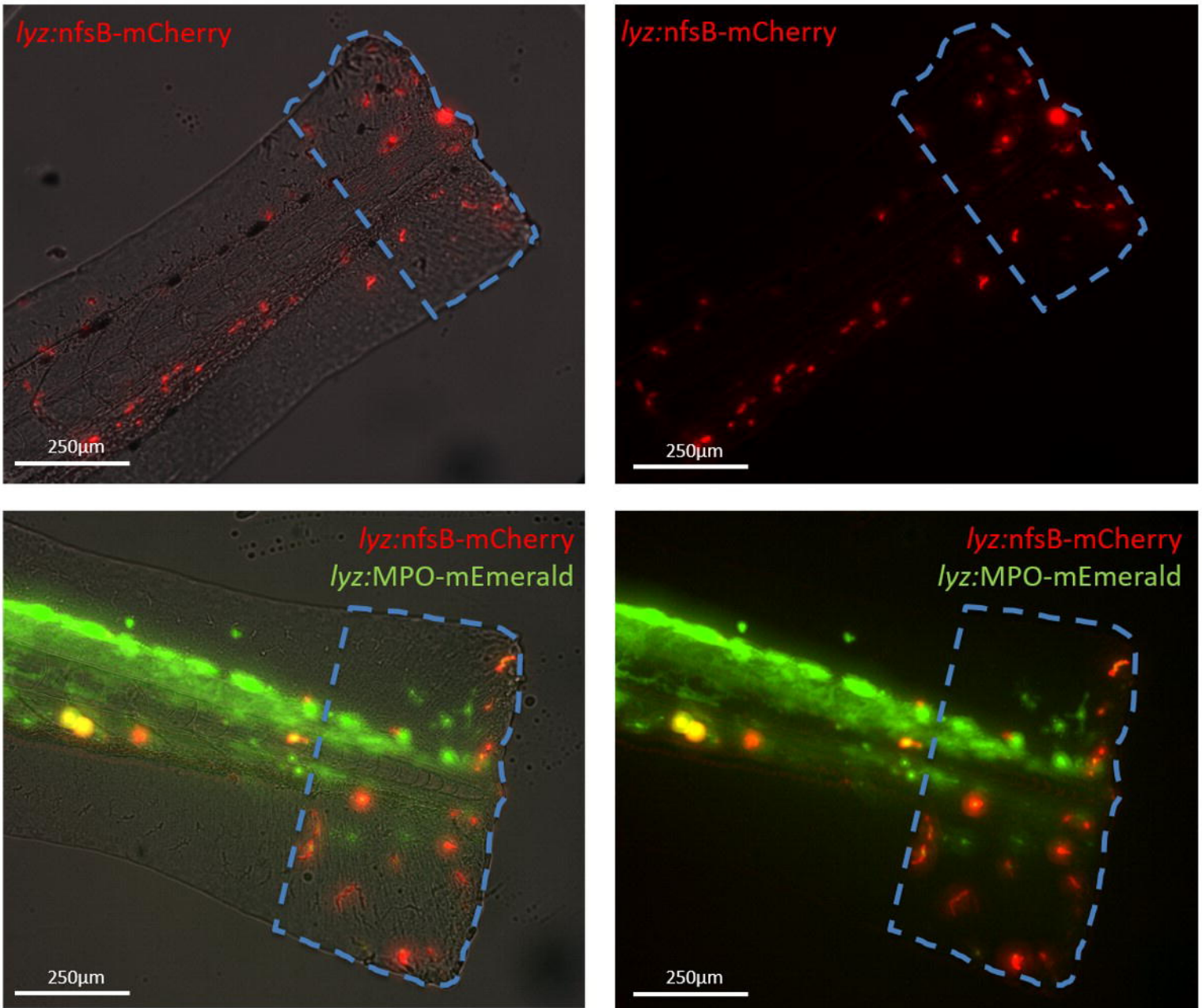


B

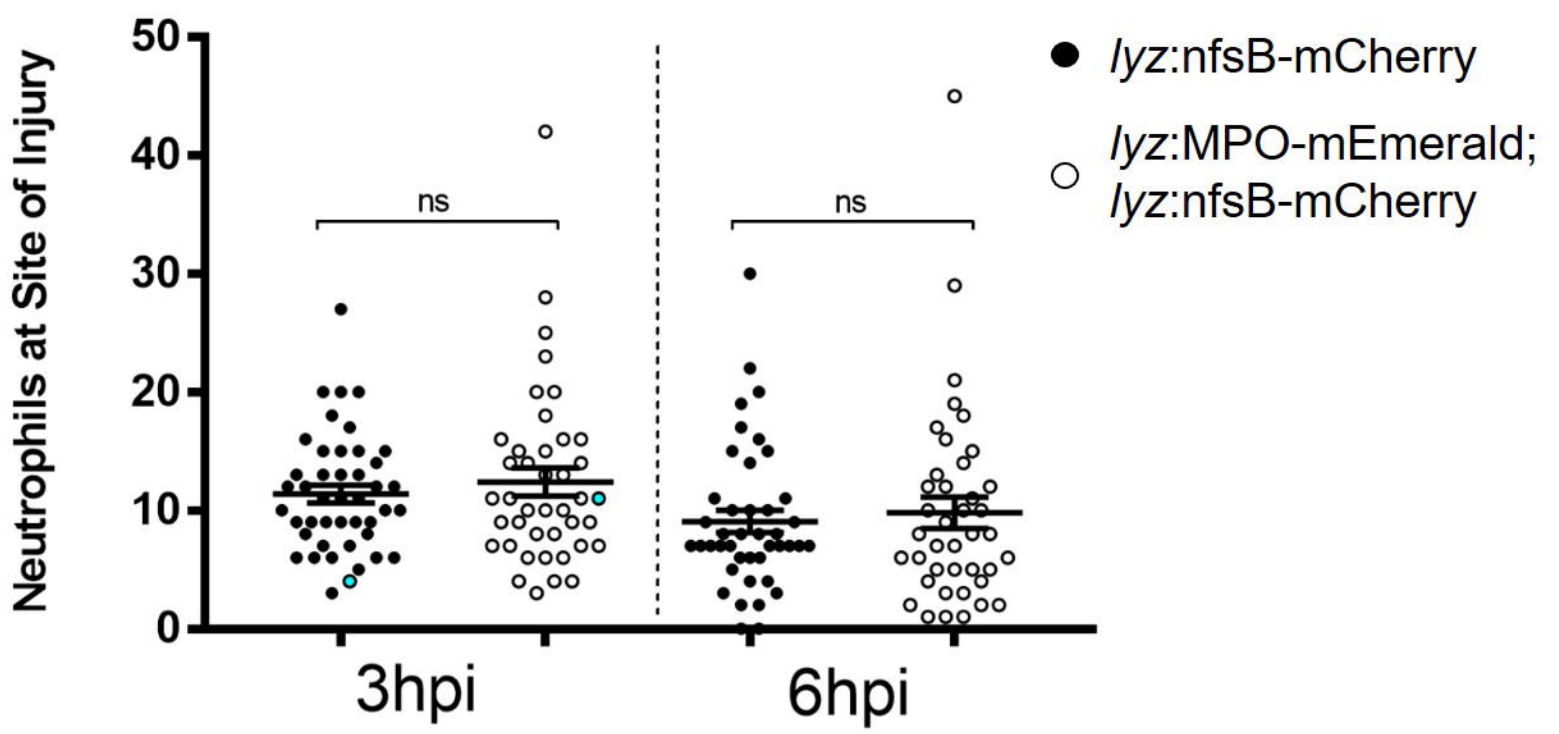




A

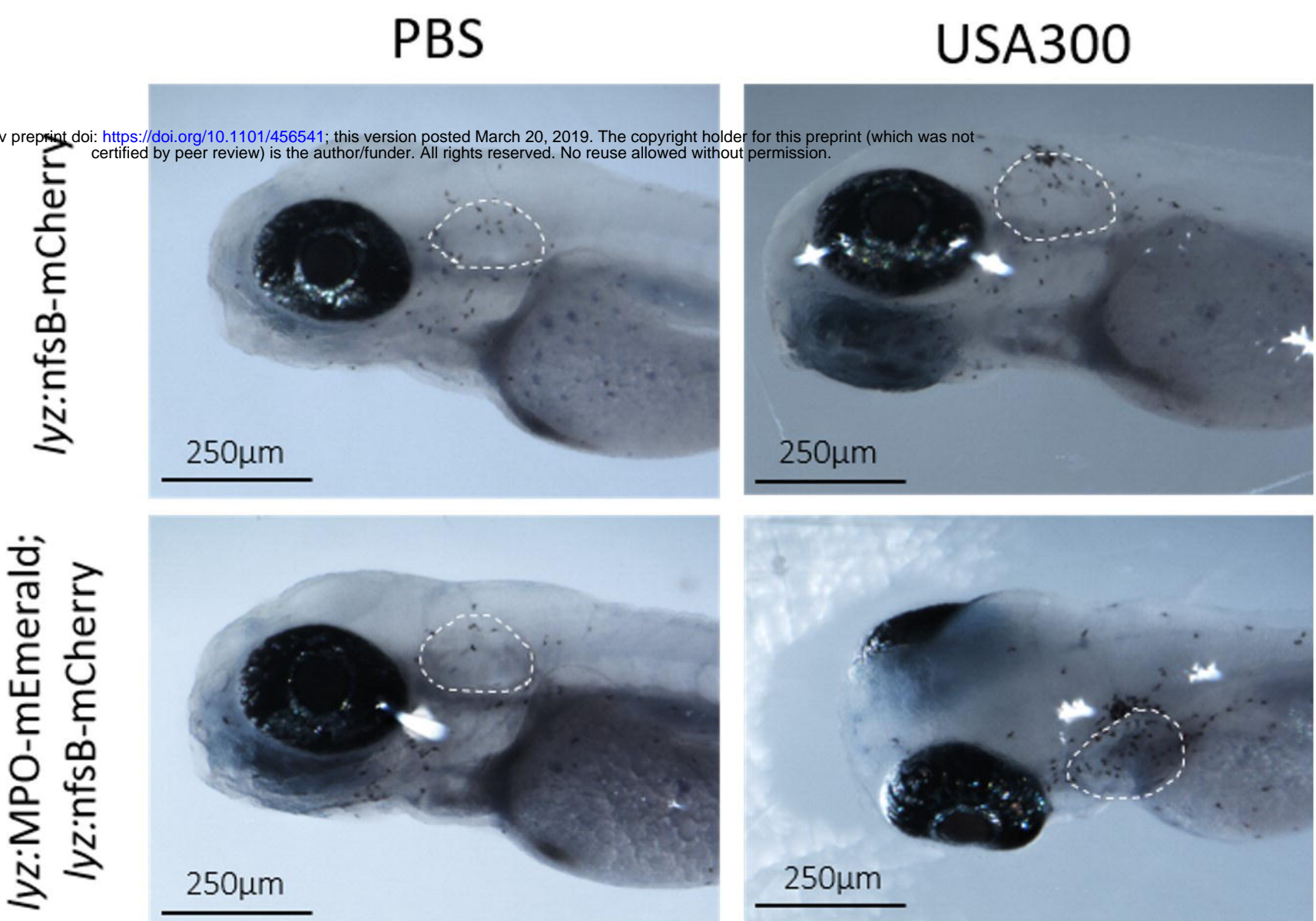


B

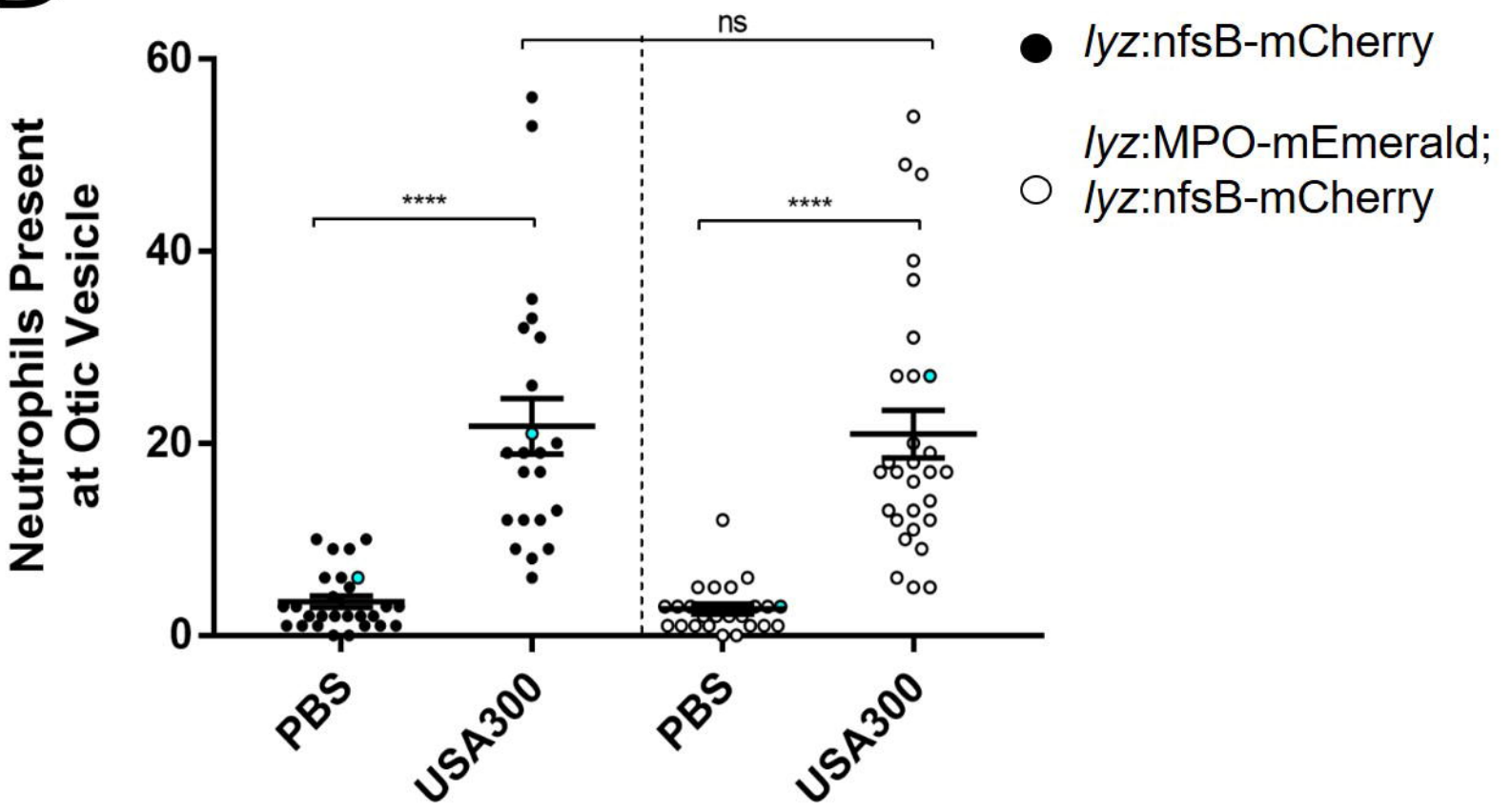


C

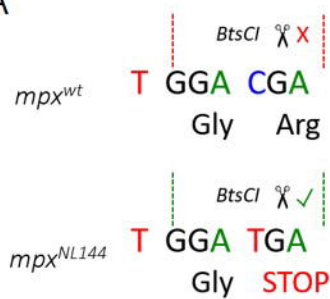
bioRxiv preprint doi: <https://doi.org/10.1101/456541>; this version posted March 20, 2019. The copyright holder for this preprint (which was not certified by peer review) is the author/funder. All rights reserved. No reuse allowed without permission.



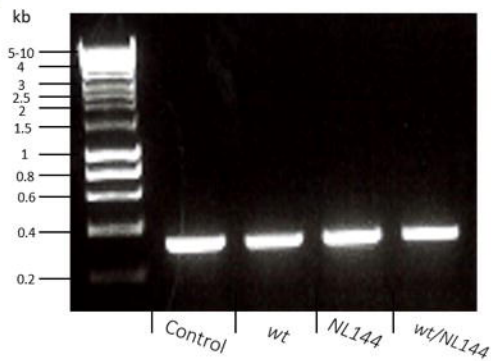
D



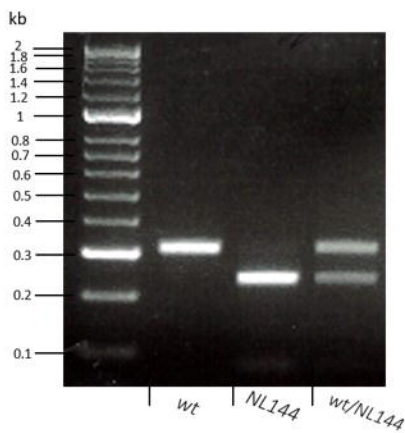
A



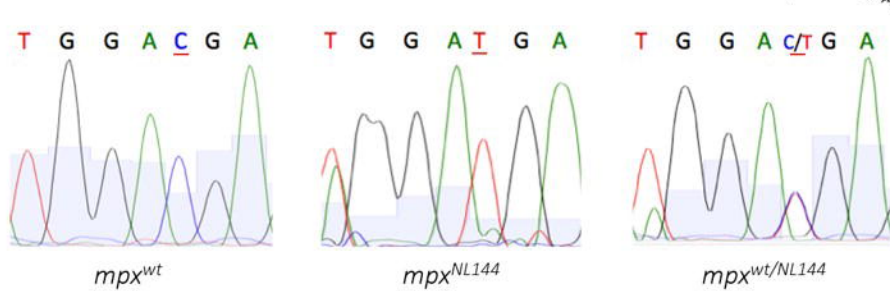
B



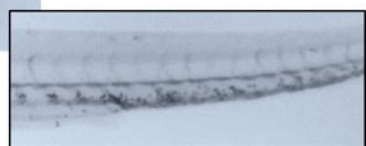
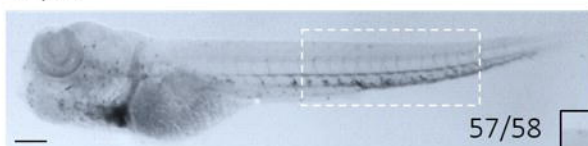
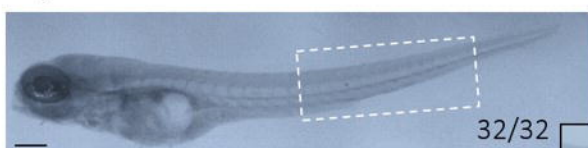
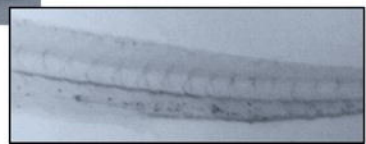
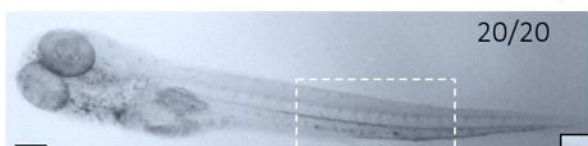
C



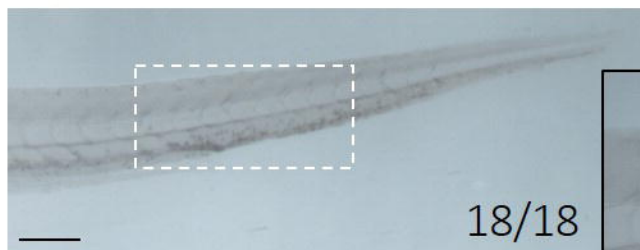
D



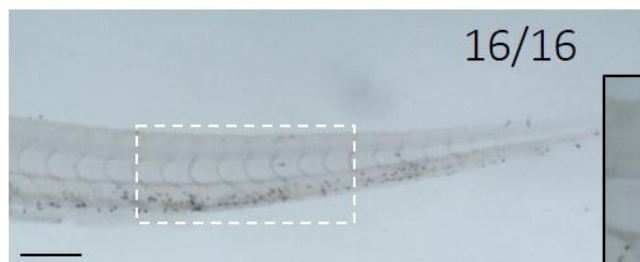
E

mpx^{wt}*mpx^{NL144}**mpx^{wt/NL144}*

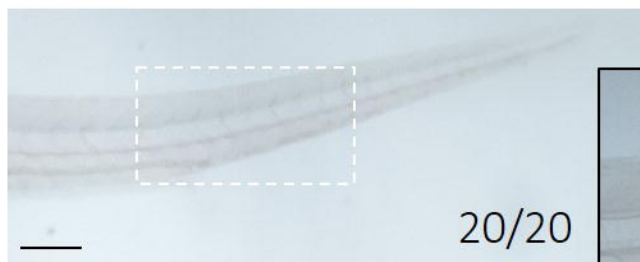
mpx^{wt/NL144}



Tg(lyz:Hsa.MPO-mEmerald,cmlc2:EGFP)sh496; mpx^{wt/NL144}



mpx^{NL144}



Tg(lyz:Hsa.MPO-mEmerald,cmlc2:EGFP)sh496; mpx^{NL144}

